Heliyon 11 (2025) e43380

Contents lists available at ScienceDirect

Heliyon

journal homepage: www.cell.com/heliyon

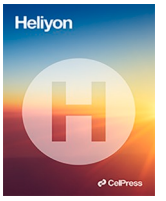

Research article

3D printed training model with sensorized arachnoid for endoscopic transsphenoidal surgery: development and initial validation

Giacomo Santona [a,*], Antonio Fiorentino [b], Francesco Doglietto [c,d], Mauro Serpelloni [a]

[a] Department of Information Engineering, Università degli Studi di Brescia, Via Branze 38, Brescia, 25123, Italy
[b] Department of Mechanical and Industrial Engineering, Università degli Studi di Brescia, Via Branze 38, Brescia, 25123, Italy
[c] Neurosurgery, Department of Neurosciences, Sensory Organs and Thorax, Università Cattolica del Sacro Cuore Rome, Largo Agostino Gemelli, 8, Rome, 00168, Italy
[d] Neurosurgery, Fondazione Policlinico Universitario A. Gemelli IRCCS, Rome, Largo Agostino Gemelli, 8, Rome, 00168, Italy

ARTICLE INFO

Keywords:
Additive manufacturing
Arachnoid membrane
Pituitary adenoma
Sensorized training model
Transsphenoidal surgery

ABSTRACT

Background: Endoscopic transsphenoidal surgery is a relatively novel technique with a long learning curve: it is used to resect tumors that grow in the sella, which is located at the center of the skull base, immediately below the optic nerves and brain that are wrapped by the arachnoid, containing the cerebrospinal fluid (CSF). One of the challenging aspects of this surgery is to remove the tumor while not damaging the arachnoid to avoid the potentially life-threatening complication of post-operative CSF leak.
Objective: This work presents the development of a new 3D-printed CT-based training model with a sensorized tank capable of reproducing the descent in the sella of the suprasellar arachnoid pushed by the cerebrospinal fluid (CSF) during removal of a sellar tumor with endoscopic transsphenoidal surgery. The system provides real-time feedback about the force exerted by the operating surgeon through the pressure sensor integrated into the tank.
Development: The model and the tank were fabricated using additive manufacturing technologies and silicone mold casting to reproduce soft tissues like skin and mucosa. The arachnoid membrane and the CSF were mimicked with a polymeric film and distilled water, while the pituitary adenoma was mimicked with boiled egg white.
Validation: The correlation between the pressure of the CSF and the exerted force was investigated in characterization tests. Eleven experienced surgeons were asked to simulate the resection of a pituitary adenoma using the model. At the end of the experience, a survey was conducted amongst surgeons to evaluate the model and its usefulness as a tool for training.
Conclusions: The collected data allowed the definition of the force threshold values for the risk of CSF leak. The maximum force exerted by surgeons is 0.526 N. Surgeons considered the arachnoid well simulated and thought that the model could be a helpful training tool for endoscopic transsphenoidal surgery.

* Corresponding author.
E-mail address: giacomo.santona@unibs.it (G. Santona).

https://doi.org/10.1016/j.heliyon.2025.e43380
Received 7 March 2024; Received in revised form 31 March 2025; Accepted 30 April 2025
Available online 5 May 2025

1. Introduction

The endoscopic transnasal transsphenoidal approach (ETA) is a new minimally invasive surgical procedure used by neurosurgeons and otolaryngologists to access the pituitary gland directly from the sella turcica to resect the pituitary adenoma (PA), a tumor that grows in the pituitary gland [1,2] and then displaces the suprasellar arachnoid and compresses the optic nerves. It is recognized that there is a steep learning curve in ETA [3], which requires specific training [4,5] to acquire specific hand-eye coordination and dexterity. One of the most delicate aspects of the surgery is the correct handling of the arachnoid membrane. The arachnoid is one of the three meninges, which are thin membranes that surround the brain and the spinal cord. From the outer to the inner one, they are called the Dura Mater, Arachnoid Mater, and Pia Mater. The arachnoid consists of two parts: the external arachnoid barrier cell membrane and the arachnoid trabeculae, a spider web-like structure [6]. Within the arachnoid trabeculae flows the cerebrospinal fluid (CSF), which is a filtered plasma solution [7], macroscopically similar to water. Concerning the mechanical properties of the arachnoid, there are no studies in the literature. The main reason is that the arachnoid and pia mater are soldered together [8], and membranes cannot be isolated and studied in a repeatable way, as stated by Walsh et al. [8]. Nevertheless, its fragility is widely recognized among surgeons, who must exercise caution when interacting with it. In fact, during tumor removal, it collapses inside the sella turcica in a sort of curtain effect due to the internal pressure of the CSF, which ranges from 10 to 20 mmHg in healthy adults [9]. So, the arachnoid may cover the remains of the tumor, and surgeons must carefully move the membrane to check for residual tumor parts to be removed. Inexperienced surgeons must learn how to perform such maneuvers safely during tumor removal to avoid damage to the arachnoid, which is associated with the potentially life-threatening complication risk of post-operative CSF leak. Training in a safe environment before entering the operating room is, therefore, fundamental for surgeons. Among all the training solutions available, the human cadaver heads remain the gold standard; their main advantage is their anatomical similarity; however, they are not an easily accessible option [5], they are expensive, and they do not usually provide simulation of pathology (e.g., sellar tumor).

In this context, the bond between additive manufacturing (AM) technologies and medicine is constantly stronger [10]. In fact, AM technologies in the medical field are used to fabricate patient-specific medical implants [10], to simulate the mechanical properties of different biological tissues [11,12], and to fabricate realistic anatomical models which can be helpful for anatomy lessons, patient information, but also for training and preoperative surgical planning [5,10]. The main reason is the possibility of obtaining complex anatomical geometries at relatively low costs [13,14]. In particular, the so-called "CT-based artificial training models", which are training models made with AM technologies and based on a Computed tomography (CT) data of a real patient, are a good alternative; their main advantage is their potential, which is inexorably linked to the complexity of the fabrication [5].

Nonetheless, the arachnoid collapse is something still unfamiliar with all the available training solutions (both commercial and experimental) [5]. In fact, the reproduction of the arachnoid membrane was only mentioned by Lin et al. [15], and it was simulated with PVCD film and water-insoluble tissue paper in a model by Harada et al. [16] for transcranial and trans-Sylvian surgery.

In this work an innovative sensorized multi-material CT-based artificial training model is presented. The goal is to give real-time feedback about the force exerted on the arachnoid membrane by the surgeon when simulating the resection of a pituitary adenoma with ETA. It is fabricated using AM and rapid tooling technologies from a CT of a real patient, the interface is modular and can be customized based on the desired case study. The model has two innovative aspects. The first one consists of a physical interface that aims at reproducing the descent in the sellar region of the suprasellar arachnoid. The second one consists of a system for the measurement of the force that the surgeon exerts on the arachnoid membrane. The tumor mass is emulated with egg white as found in the literature [17–22] and according to surgeons experience as reported in our previous work [23,24]. Furthermore, in this work, a first validation with experienced surgeons is presented. A pool of 11 experienced surgeons, both neurosurgeons and otolaryngologists, tested the model and provided on field measures on the exerted force and their surveyed opinions.

2. Materials and methods

2.1. Design and fabrication of the training model

The training model consists of two modules: a CT-based anatomical module and a sensorized tank module. The CT-based anatomical module is developed starting from the CT data of a patient and faithfully reproduces the narrow geometry of the face, the nasal cavities, and the sellar region. The anatomical module replicates the patient-specific case study and can be fully customized based on training purposes. The sensorized tank module is mounted on the anatomical model and integrates a pressure sensor that allows data collection during the surgical procedure thanks to a measurement system. The tank system replicates the fall of the arachnoid within the sellar region during removal of a large pituitary adenoma. It is screwed to the frame module just above the sphenoid bone to faithfully reproduce the position of the arachnoid membrane in relation to a pituitary tumor. This is one of the most important innovations introduced in the model from a surgical simulation point of view, as none of the available training models or simulators reproduce such feature [5].

2.1.1. CT-based anatomical module

The CT-based anatomical model was specifically designed for ETA training. The model was designed starting from a patient's CT data. The CT was performed using a 1×1 frame with contiguous slices, at 1.5 mm. CT was performed at a gantry of 0°, with a scan window diameter of 225 mm and a pixel size of more than 0.44×0.44. Images were recorded on a CD in DICOM format. In the first step of the elaboration, with Autodesk Meshmixer (Autodesk, Inc., USA), the volume of interest was isolated, and the rest was removed according to the fact that, during the surgery, only the nose and the area around are visible while the rest is covered. Following the

material-saving principle, everything that falls outside the visible area was removed. In the second step of the elaboration, a modular structure was designed by cutting the "skull-base" model. Three parts were obtained: the ethmoid bone, the nasal cavities, and the sphenoid bone, which was further divided into two parts, the sellar region and a lower part, as a mechanical support. Fig. 1 shows the results of the face (Fig. 1a), and the skull-base region divided into sphenoid bone, nasal cavities, and ethmoid bone (Fig. 1b). In particular, the face of the patient used in this work has been edited with Meshmixer in such a way that it is not recognizable. In the third step of the elaboration, the single parts of the anatomical module were identified and designed: face (skin and ethmoid bone), turbinates (only the inferior and the middle were simulated), nasal septum, frame, and sphenoid bone. Fig. 2 provides an exploded view of the computer-aided design (CAD) model of the training model, which includes the sensorized tank module where the arachnoid and the CSF are contained. A detailed description of the tank module can be found in the following section 2.1.2, entitled "Sensorized tank module."

Each part of the anatomical module was 3D printed on an Ultimaker 3 Extended (Ultimaker, Netherlands) in PLA, except for the nasal septum, which was 3D printed in TPU 95A to better mimic the flexibility of the cartilage. Both filaments have a diameter of 2.85 mm and were printed using an AA 0.4 print core. The soft tissues of the mucosa and the skin were fabricated by mold-casting silicone into silicone molds to reduce the extraction problems of undercuts. Parts that were 3D printed in PLA were used as patterns to shape the molds. An example of the procedure is reported in Fig. 3. The figure shows the three phases of silicone model making: (1) design of the CAD model, Fig. 3a, (2) preparation of the casting molds, Fig. 3b and (3) the final product removed from the mold after the silicone has cured, Fig. 3c. The face module was designed together with the ethmoid bone inserted. Moreover, two removable nostril mold-cores recreated the nostrils (Fig. 3a). Casting molds were fabricated using Mold Star ™ 15 SLOW silicone (Smooth-On, Inc., USA), while parts (skin and mucosa) were fabricated using Dragon Skin ™ 30 silicone (Smooth-On, Inc., USA) silicone mixed with Silc Pig ™ "Light Flesh" colored pigment (Smooth-On, Inc., USA), to improve the realism of the skin and the mucosa. Before pouring, silicones were degassed at 90 % vacuum to remove entrapped air. Moreover, Ease Release ™ 205 (Smooth-On, Inc., USA) agent was used to keep the surfaces of the parts separated where required.

The fabrication procedure consists of the positioning of the pattern on a clay base (Fig. 3b) and the pouring of the first half of the silicone mold. After curing, the clay is removed, and the second half of the mold is cast above the first one. Then, inserts and cores are positioned if required, and the Dragon Skin ™ 30 silicone for the parts is poured. Fig. 3c reports the obtained face module once extracted from the mold with embedded ethmoid bone and nostril cavities. Table 1 presents a summary of the fabrication technologies, and the material selected for each module.

2.1.2. Sensorized tank module

The sensorized tank module aims to train surgeons to handle the collapse of the arachnoid correctly during tumor removal and to avoid its damage. As suggested by Harada et al. [16] and in collaboration with expert surgeons, a polymeric film membrane (Domopak food film, Cuki Cofresco S.r.l., Italy) was considered the best alternative to mimic the thickness and the transparency of the arachnoid membrane, as we previously reported [25]. Concerning the liquid used to emulate the CSF, which is 99 % water [26], not much different from saline solution [27–31], distilled water was used, as previously reported [25]. Hence, the tank was designed according to the previous considerations, to fit the upper sphenoid bone module so that the polymeric film fits within the sella turcica. Fig. 4 shows two CAD models: the first is an exploded view of the tank (Fig. 4a), and the second is the entire tank mounted (Fig. 4b). The tank consists of a base plate, two columns, a membrane, a gasket, a sealing plate, and a pressure sensor (Fig. 4a). The idea is to wrap the polymeric film around a U-shaped structure (base plate and columns) to shape the polymeric film. Moreover, two lateral supports connected to the tank through dovetail joints were added to keep the model in a position similar to the patient during the surgery, which is typically positioned supine with the head elevated up to approximately 30° [32]. The sensor is connected to the sealing plate with a PVC tube to one of the lateral supports, which is equipped with two clips to hold the sensor at a constant height during tests. Finally, two additional tubes were added to insert the liquid and let the air out.

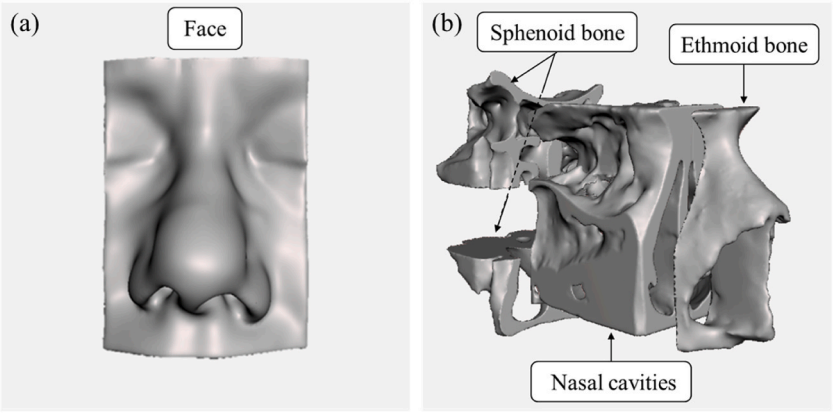

Fig. 1. Design of the CT-based anatomical model. Anatomy of the face module (a) and the "skull-base" model with sphenoid bone, nasal cavities, and ethmoid bone modules (b).

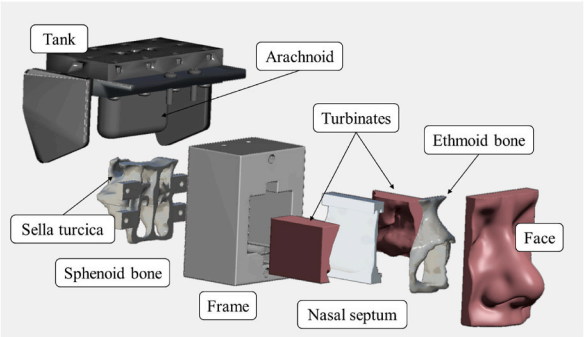

Fig. 2. Exploded view of the CT-based anatomical model.

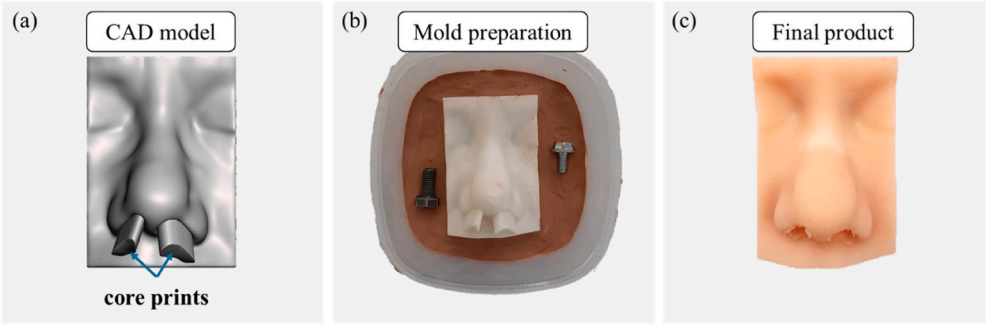

Fig. 3. Design of the patterns for silicon casting. (1) CAD model of the face with core prints into the nasal cavities (a). (2) Mold preparation: the 3D printed face module inserted into clay as a pattern for the mold (b). (3) Final Product: the face module removed from the mold after the silicone has cured (c).

Table 1
Summary of the technologies and materials adopted to fabricate the parts of the CT-based anatomical module.

Part	Technology	Material
Face	FFF + Mold Casting	Silicone - Dragon Skin ™ 30
Cores (Nostrils)	FFF	Pearl-White PLA
Ethmoid bone	FFF	Pearl-White PLA
Nasal septum	FFF	TPU 95A
Turbinates	FFF + Mold Casting	Silicone - Dragon Skin ™ 30
Frame	FFF	Pearl-White PLA
Sphenoid bone	FFF	Pearl-White PLA

The tank was printed in ABS on a Stratasys Dimension 1200es (Stratasys, Inc., USA), except for the TPU gasket, which was printed on an Ultimaker 3 Extended. Indeed, the mechanical properties of TPU make it a more suitable material for use as a gasket. Additionally, the two columns were covered with shrinkable thermoplastic strips to prevent the polymeric film from tearing by friction. Furthermore, to improve the airtightness of the sealing plate, it was painted with three layers of liquid rubber.

The pressure sensor integrated into the sealing plate between the two tubes measures the variation of the differential pressure between inside and outside the tank. When a force is applied to the membrane, a deformation of the membrane itself is generated, and a variation in the pressure difference can be measured. The pressure sensor is the 24PCEFA6D by Honeywell (Honeywell International, Inc. USA), and it has a full Wheatstone bridge configuration. It has a full-scale value is 3.447 kPa, a sensitivity of 0.100 kPa/mV and $\pm$0.050 kPa of repeatability and hysteresis.

2.2. Characterization of the sensorized tank

A specific electronic setup has been used for the estimation of the force applied by a commercial load cell to the membrane, achieved through the measurement of the pressure sensor integrated into the tank. The intention is to use an indenter, a curette, to exert force against the membrane, to increase the internal pressure of the tank. A curette is a spoon-like instrument commonly used in various surgical procedures. During ETA, it is employed by surgeons a ring-shaped tip curette with an external diameter of 2 mm for several applications, including: navigating through the nasal cavity, removing the pituitary tumor, moving the arachnoid membrane,

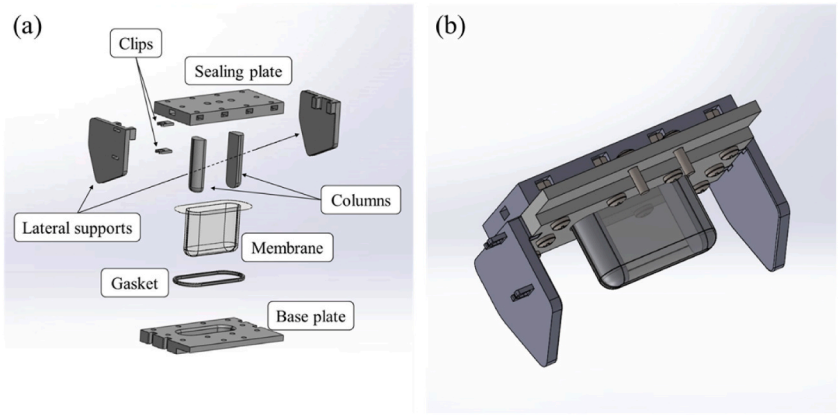

Fig. 4. CAD model of the tank. Exploded view of the tank system (a) and the assembled tank (b).

and checking for residual tumor remnants. The curette is mounted on a micrometric slide for its movement during tests. The micrometric slide is computer-controlled with a dedicated software, it has a full-scale value of 25 mm and a resolution of 10 μm. In addition to displacement, the user can indicate the direction, speed, acceleration, and number of repetitions of the movements. The micrometric slide has an embedded commercial load cell which measures the force. The commercial load cell, as resulted in previous characterization [25], has a sensitivity of 4.353 N/mV. It is used to measure the force exerted by the curette on the polymeric membrane. As already mentioned, the pressure of the distilled water within the tank is measured by a pressure sensor. The sensor signal is conditioned by a custom electronic module for Wheatstone Bridges at 10 V. Data from both sensors were elaborated by a conditioning electronic circuit, the output signals were collected with an HP34401 multimeter (Hewlett-Packard, USA) for each sensor, with a resolution of 6 ½ digits. Furthermore, the two multimeters are linked to the PC via the same GPIB-USB-HS interface, allowing for the simultaneous collection of both sensor signals. This facilitates the immediate correlation of data from the load cell to the pressure sensor. The PC is than interfaced with a LabVIEW program (National Instruments, USA) using 1 Hz as a sampling rate. Data are then analyzed on specifically designed MATLAB (MathWorks, USA) programs. Fig. 5 shows the electronic setup used during the characterization tests.

The characterization of the measuring system consisted of a set of indentations performed on the membrane using a curette with the already mentioned characterization setup. The curette was mounted on the micrometric slide facing the training model, so to replicate the movement during the actual surgical procedure. Tests were conducted at a constant depth of penetration in the membrane, and 7 subsequent repetitions were conducted. A total of 8 depths ranging from 1 to 15 mm were considered and repeated three times during different days. Each of these three replications were performed changing each time the membrane, to prevent any potential alteration of the results due to membrane damage. Preliminary analysis showed that the filling procedure of the tank is crucial to ensure the

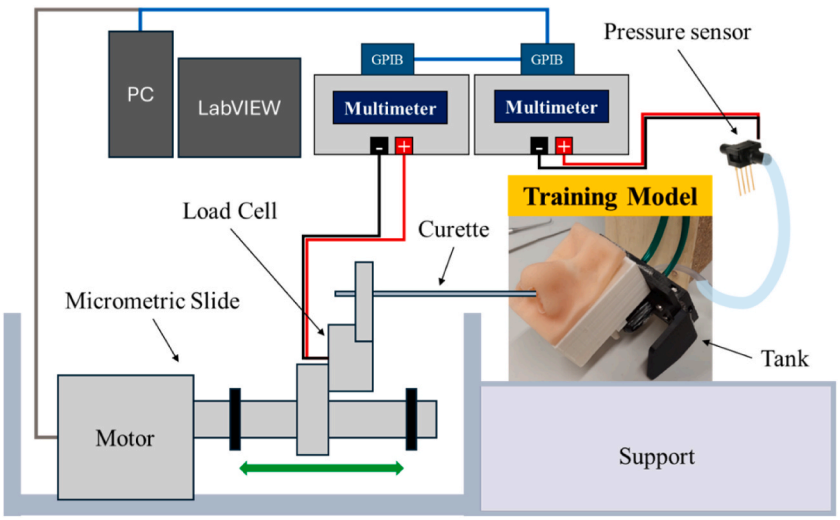

Fig. 5. The electronic setup. A curette is moved by a micrometric slide with a load cell embedded, which presses the membrane of the tank. The imposed stress causes an increase in the inner pressure of the tank, which is read by the pressure sensor connected to it. The data are then collected by a LabVIEW program and analyzed with the MATLAB software.

repeatability of the tests (i.e., each time the membrane is replaced). It was observed that the amount of liquid, in conjunction with the presence of air within the tank, can influence the haptic feeling of the membrane. This affects the variation of the inner pressure during indentation, and subsequently the outcome of the tests. Hence, a filling protocol was defined, in accordance with an experienced surgeon, to replicate the membrane rigidity. Within the protocol, the sensorized tank is filled with distilled water through one PVC tube until the total amount of water reaches 30 g. Exceeding water and entrapped air are removed through the second tube. With this setup, the behavior of the film is similar to the arachnoid membrane.

2.3. Surgeon experience and feedback

Once the tank system was characterized, the training model was assessed by 11 international surgeons (3 neurosurgeons and 8 otolaryngologists) with an experience in ETA ranging from 3 to 20 years reported in Table 2. Surgeons were invited to participate in an in-field test of the training model, simulating the resection of a pituitary adenoma. During these simulations, a boiled egg white was used to mimic the consistency of a pituitary adenoma. The idea came from a particular group of the artificial training model found in the literature called “EggHead” which is characterized by the usage of a boiled chicken or quail egg to mimic the sella turcica and its content [17–22].

The surgical simulation was conducted using surgical instruments: the endoscope, the aspirator, and the curette. An additional test was conducted using an alternative technique, which involved the use of a cotton gauze between the curette and the arachnoid membrane. This test was performed to compare the effects of the different techniques. Data on pressure and force applied to the membrane during the surgery were collected and then analyzed using MATLAB. To remove sensor noise, data were initially filtered according to a threshold value of 0.1 N, which was determined to be a minimum threshold value. The threshold was chosen in accordance with the results obtained by Bekeny et al. [33] where the minimum force reported on soft tissue was of 0.1 N during a real transsphenoidal surgery. During the testing phase, each instance of interaction between the surgeon and the arachnoid membrane was registered as a peak by the pressure sensor mounted on the training model. Each peak prominence, calculated using the MATLAB function *findpeaks*, was subjected to analysis. The prominence of a peak is defined as the difference between the height of the peak and the lowest point in the nearest valley separating that peak from another higher peak. Results were employed in the estimation of a threshold value above which the force applied is statistically likely to result in the tearing of the membrane. In section 3.3 entitled "Surgeons Experience”, results will be presented.

Furthermore, surgeons were surveyed at the end of the simulation to collect their feedback on the realism and utility of the training model, the questionnaire is reported in Table 3. A total of nine questions were asked: three questions were about the arachnoid, four questions were about the adenoma, and two questions were about the usefulness of such a training model. Q1 and Q2 ask to evaluate the anatomical realism of the arachnoid, especially regarding its deformability and force resistance. Q3 is about its overall haptic behavior. Q4, Q5, and Q6 evaluate the anatomical realism of the mimicked pituitary adenoma in terms of its removability, deformability, and mechanical feedback. Q7 is about its overall similarity to the real tumor.

3. Results

3.1. Development of the training model

The CT-based anatomical model is assembled and reported in Fig. 6. The turbinates and the nasal septum are inserted into the frame (Fig. 6a), the face is mounted to the front of the frame (Fig. 6b), and the sphenoid bone is fastened to the back of the frame (Fig. 6c). Fig. 7 shows the CAD model of the tank (Fig. 7a) and the sensor-equipped tank mounted and filled with water (Fig. 7b). Additionally, Fig. 7b shows the tubes included in the tank: the filling tubes and the sensor tube. Filling tubes are used to introduce distilled water into the tank and to remove air, while the sensor tube is used to connect the sensor to the tank. Fig. 8 compares the CAD model (Fig. 8a) with the assembled training model (Fig. 8b), which is ready to be used for surgical simulation.

Table 2
Surgeons participating in the field testing. (YoE = Years of Experience).

#	Country	Specialty	YoE
1	Italy	Otolaryngologist	15
2	Albania	Otolaryngologist	12
3	France	Neurosurgeon	20
4	Italy	Otolaryngologist	15
5	France	Otolaryngologist	3
6	Argentina	Otolaryngologist	15
7	Italy	Otolaryngologist	13
8	Italy	Neurosurgeon	14
9	Türkiye	Otolaryngologist	10
10	Italy	Otolaryngologist	15
11	Italy	Neurosurgeon	20

Table 3
The questionnaire submitted to surgeons.

Topic	Question					Answer type
Arachnoid	Q1	How do you evaluate the deformability of the arachnoid compared to the real one?				Type 1
	Q2	How do you evaluate the force resistance of the arachnoid compared to the real one?				Type 1
	Q3	Overall, how much do you think that the haptic feedback of the arachnoid is similar to the real one?				Type 2
Tumor	Q4	How do you evaluate the removability of the pituitary adenoma compared to the real one?				Type 1
	Q5	How do you evaluate the (consistency) deformability of the pituitary adenoma compared to the real one?				Type 1
	Q6	How do you evaluate the force resistance of the pituitary adenoma compared to the real one?				Type 1
	Q7	Overall, how much do you think that the pituitary adenoma is similar to the real one?				Type 2
General	Q8	Do you think that an instrumented training model for endoscopic transsphenoidal surgery could be useful?				Open-ended
	Q9	Do you have any suggestions?				Open-ended
Answer Type 1		−2	−1	0	+1	+2
		Lower	Slightly lower	Neutral (goal)	Slightly higher	Higher
Answer Type 2		1/5	2/5	3/5	4/5	5/5
		Strongly Disagree	Disagree	Neutral	Agree	Strongly Agree

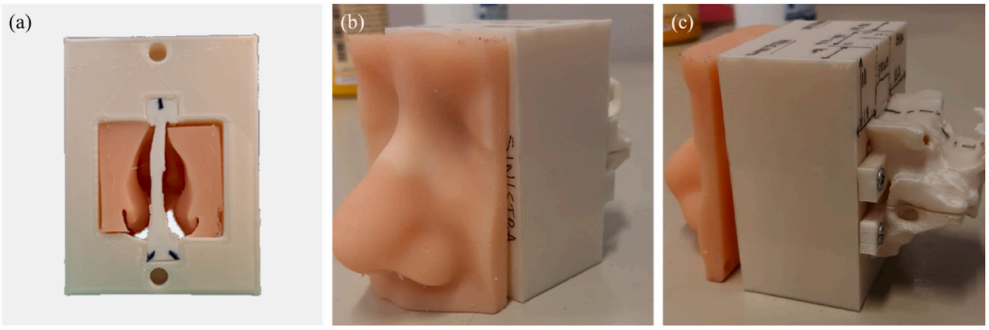

Fig. 6. The CT-based training model. An interior view of the model shows the positioning of the turbinates and the nasal septum modules within the frame module (a). Overview of the assembled training model (b and c).

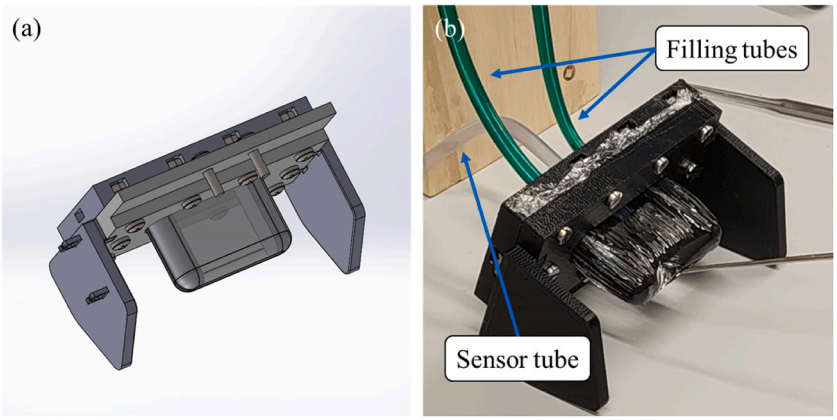

Fig. 7. The tank system mounted. Comparison between the CAD model (a) and the tank filled following the "filling protocol" (b). Filling tubes are used to introduce distilled water into the tank and to remove air, while the sensor tube is used to connect the sensor to the tank (b).

3.2. Characterization of the sensorized tank

For each repetition, the values of the peak prominence of force and pressure were recorded. The overall data show a linear correlation between Force and Pressure with an R^2 of 0.972 and a sensitivity of the measuring system of 1.289 N/kPa. The linear correlation found, shown in Fig. 9, was used to convert pressure data from the pressure sensor into force, i.e., the force applied to the membrane.

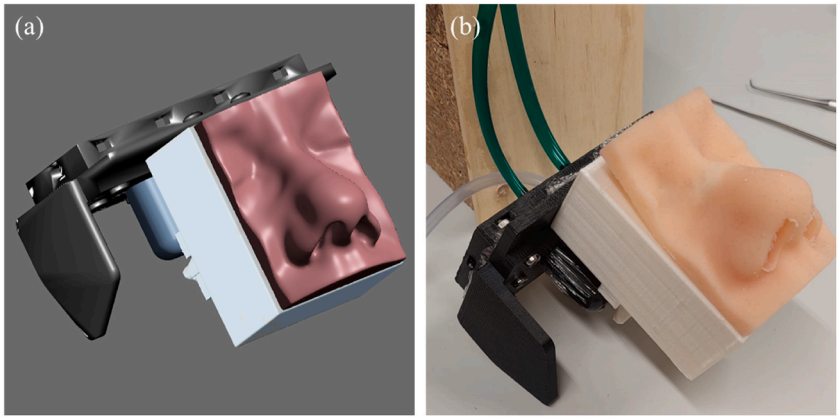

Fig. 8. CT-based training model. Comparison between the CAD model (a) and the CT-based anatomical model ready for a simulation (b).

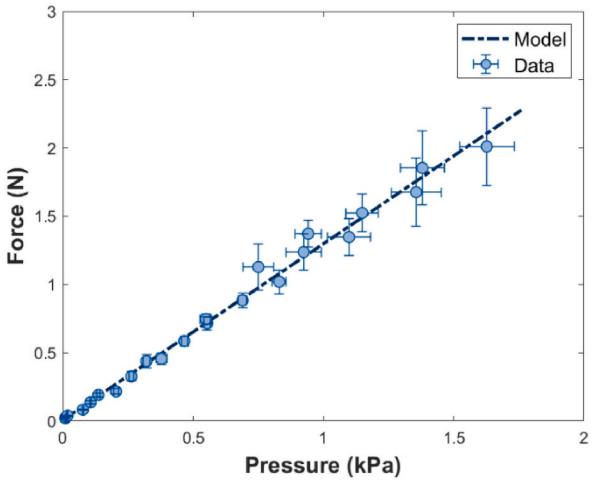

Fig. 9. Results of the characterization tests. Correlation between force (N) and pressure (kPa) values obtained through the characterization tests conducted on the tank. The tests consisted of repeated indentation at varying displacement of the micrometric slide. The resulting model was found to be linear, with an R^2 value of 0.972 and a sensitivity of 1.289 N/kPa.

3.3. Surgeons experience

Before testing with experienced surgeon, the upper sphenoid bone module of the training model was drilled to expose the arachnoid membrane. In addition, in sake of simplicity, the turbinates and nasal septum modules were removed during surgical simulations. Tests were conducted with the experienced surgeons reported in Tables 2 and in an anatomical laboratory with surgical instruments, as shown in Fig. 10. The egg white specimen was inserted into the sella turica to mimic the tumor, resulting in an initial compression of the membrane. Fig. 11 shows the outcome for one surgeon, data are already converted from kPa to N with the linear model described in section 3.2 "Characterization of the sensorized tank". Tests were also conducted with a cotton-gauze. Fig. 12 shows two images taken with the endoscope for both techniques: stand-alone curette (Fig. 12a) and curette with the cotton gauze (Fig. 12b).

To evaluate the stresses acting on the membrane during the surgical procedure, as mentioned in the previous section 2.3 entitled "Surgeon experience and feedback", peak prominence values were considered and analyzed for every surgeon combined. Then, their mean and standard deviation values were estimated, $\mu = 0.230$ N and $\sigma = 0.099$ N, respectively. These values were used to define three working areas based on the surgical risk (Fig. 13a). Similarly, the results of the test performed using the cotton gauze between the curette (Fig. 13b) and the membrane were elaborated. Their average and standard deviation are $\mu = 0.280$ N and $\sigma = 0.170$ N, respectively. A summary of the results can be found in Table 4, where are confronted with results found in literature [33].

3.3.1. Questionnaires

Results of the questionnaires are reported in Fig. 14, divided by medical surgeon's specialty: Neurosurgery – Ns – and Otolaryngology – Ot –. It is possible to observe that the mechanical behavior of the membrane (Q1 and Q2) and the tumor (Q4, Q5, and Q6) are close to the goal (neutrality to actual tissues), as illustrated in Fig. 14a. Overall, Q3 and Q7 suggest that some aspects of the model

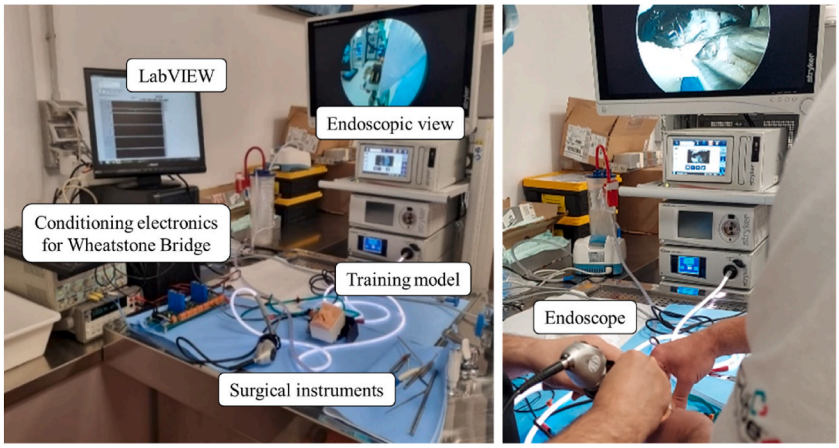

Fig. 10. The experimental setup during the field testing with experienced surgeons.

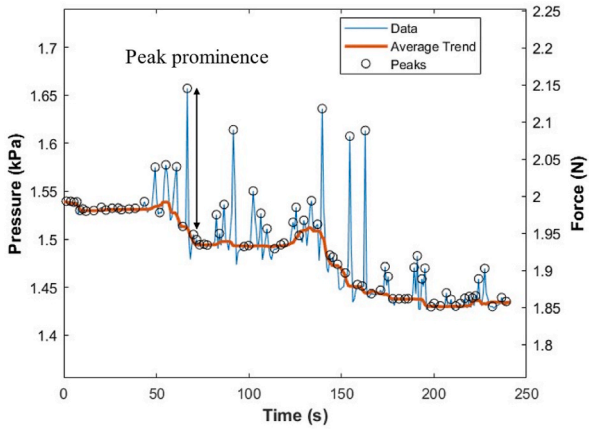

Fig. 11. Example of a tumor removal performed by an experienced surgeon. The tumor removal is measured and reported (blue line). Removing the tumor causes here an average decreasing trend (red line). Local peaks are a consequence of the compression of the membrane by the curette (black circles). The peak prominence was calculated using the MATLAB function *findpeaks*.

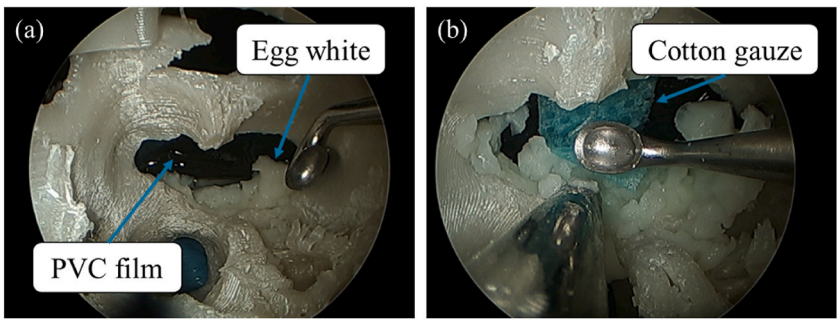

Fig. 12. Endoscopic view of the field tests with experienced surgeons. Removal of the tumor with a curette with the arachnoid partially falling and covering the adenoma (a). The same procedure was performed, but a cotton gauze was placed between the curette and the membrane (b).

should be improved to get closer to reality, as illustrated in Fig. 14b. In particular, the open-ended answers Q8 and Q9 explain that the improvements should involve the following aspects.

- The arachnoid could be looser and thinner.

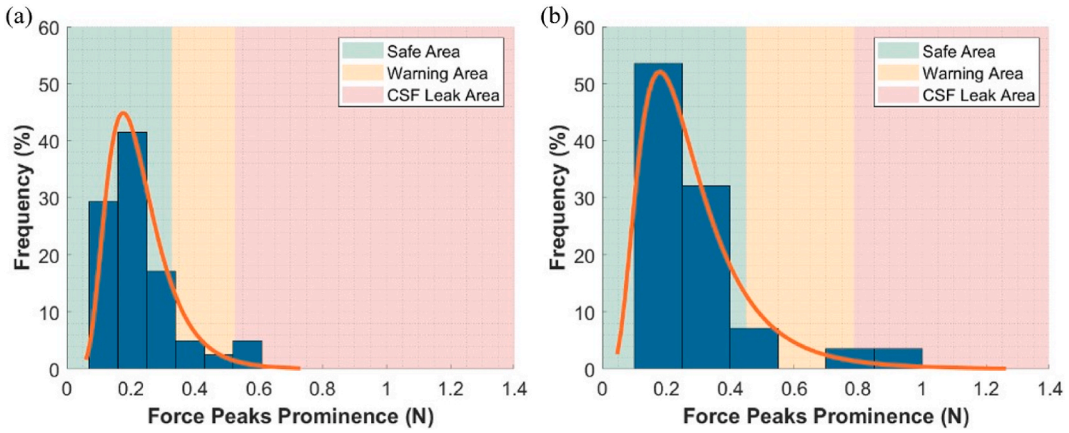

Fig. 13. Histograms of the force peak prominence values. Without the cotton gauze (a) and with the cotton gauze (b). Three working areas were defined based on the surgical risk: the Safe Area (up to $\mu + \sigma$), the Warning Area (between $\mu + \sigma$ and $\mu + 3\sigma$), and the CSF Leak Area (over $\mu + 3\sigma$). The safe area was found to be wider when using the cotton gauze.

Table 4
Ranges of the Safe, Warning, and CSF Leak Areas for the Force applied on the membrane, compared with data available in the literature [33].

Data	Unit	Technique	Safe Area	Warning Area	CSF Leak Area
Bekeny et al. [33]	N	Sensorized Curette	0.100 ÷ 0.500	–	–
Force (our results)	N	Curette	0.100 ÷ 0.328	0.328 ÷ 0.526	>0.526
Force (our results)	N	Curette and Cotton Gauze	0.100 ÷ 0.450	0.450 ÷ 0.618	>0.786

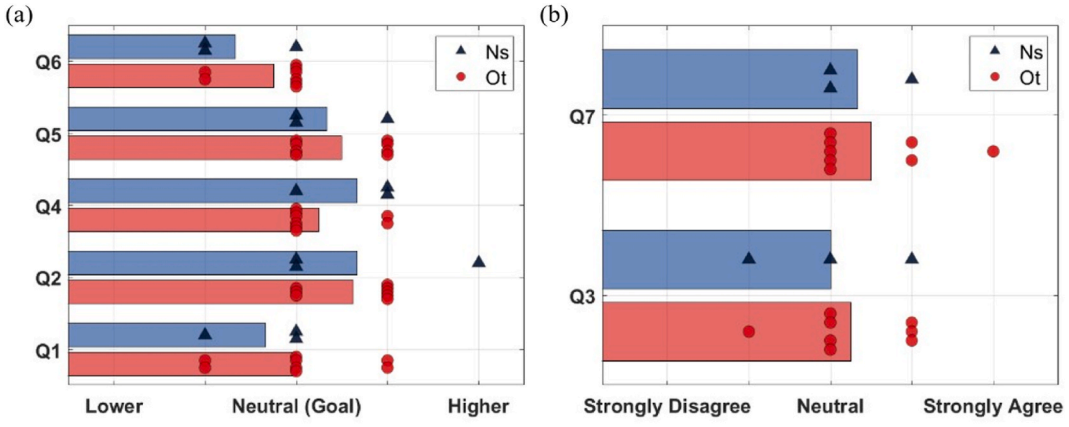

Fig. 14. Results of the questionnaire. Answers are divided by medical specialty, Neurosurgery (Ns), and Otolaryngology (Ot). The mechanical behavior of the membrane (Q1 and Q2) and the tumor (Q4, Q5, and Q6) are close to the goal (neutrality to actual tissues) (a). Q3 and Q7 suggest that some aspects of the model should be improved to get closer to reality (b).

- The tactile feedback of the adenoma is optimal, but different consistencies should be provided (softer and harder). Moreover, its fragility-deformability when curetting is different as the tissue breaks in larger parts. Its "liquidity" should be increased.
- Colors in the model and bleeding should be included.

4. Discussions

The model presented in this work effectively represents the narrow anatomy of the skull base, as indicated by the questionnaire results, it lacks some anatomical parts such as the internal carotid artery, the optic nerves or the bleeding effect, which would improve the realism during the simulation and be a more functional tool for surgeons trying for the first time such a complicated surgery.

Regarding the sensorized tank, the characterization of the pressure sensor reported in Fig. 9 reveals a clear linear correlation between force and pressure, although the dispersion of data increases for values of pressure exceeding 1 kPa. The resulting

characterization model was used to convert the data from pressure to force to verify that they were consistent with the work found in the literature. The standard deviation of pressure values ranges from <0.001 at 0.010 kPa to 0.105 at 1.627 kPa, while the standard deviation of the force ranges from 0.001 at 0.032 N, to 0.284 at 2.011 N.

With the sensorized tank mounted on the training model as shown in Fig. 8, tests were performed with experienced surgeons (both Neurosurgeons and Otolaryngologists) in the anatomical laboratory as shown in Fig. 10. A removal of PA with ETA was simulated using an egg white sample used to mimic the pituitary adenoma as suggested by literature [17–22] and by our former experience [23, 24]. Surgeons were asked to remove the egg white as in a real ETA surgery while the force exerted on the sensorized tank mimicking the arachnoid membrane was measured. The profile of the surgery force outcome of a surgeon is shown in Fig. 11. As it can be seen, the system registers an initial compression, as caused by the egg white sample inserted into the model which compresses the arachnoid membrane. The trend of the surgical test shown in Fig. 11 is decreasing, since the removal of the egg white specimen slowly decompresses the membrane thus reducing the overall internal pressure in the tank. Two different techniques were tested: one using a stand-alone curette and the other employing cotton gauze, as illustrated in Fig. 12. The gauze, when inserted over the arachnoid membrane, allows the surgeon to distribute the pressure exerted by the surgical instrument to a wider area, thereby increasing the range of forces that can be applied. This is evident from Table 4, which shows that the mean value of surgical simulation with the gauze is higher. In addition, the force limit of the CSF Leak Area is 49 % higher. Hence, a higher force is permitted during the surgical procedure without increasing the risk of arachnoid damage. From the results emerges that both tests configuration: stand-alone curette and with the cotton gauze, follow a log-normal distribution with a p-value of 0.972 and 0.550 respectively, the p-value was calculated using the one-sample Kolmogorov-Smirnov test, with the MATLAB function *kstests*. As already mentioned in section 3.3 entitled "Surgeons Experience" three different area, according to the surgical risks were defined: the Safe Area (green) for force values lower than $\mu + \sigma$, the Warning Area (yellow) for forces between $\mu + \sigma$ and $\mu + 3\sigma$, and the CSF Leak Area (red) for forces greater than $\mu + 3\sigma$. The Safe Area represents those values of force that were considered safe during the simulation. The Warning Area represents those values that are close to the breaking of the membrane. The CSF Leak Area contains the highest force values, which are associated with the rupture of the arachnoid membrane for the patient. The force limits of the three areas were compared with the ones present in the literature (Table 3). In the work of Bekeny et al. [33] measured the force exerted by surgeons during a transsphenoidal surgical approach with a sensorized curette; as a result, the force exerted on soft tissues ranges from $0.1 \div 0.5$ N, which corresponds to the values of Safe and Warning Areas together. Even though there is no experimental validation of the limit values found here, they are reasonable. Further investigation will define their values better. When comparing the results of the stand-alone curette technique (Fig. 13a) and the cotton gauze technique (Fig. 13b) is clear that the force limits of the working areas are higher than when the curette alone is adopted.

In conclusion, this work presents the development of a new multi-material modular CT-based training model for simulating the endoscopic transnasal transsphenoidal surgery approach to resect pituitary adenomas. Its innovative features consist of the emulation of the arachnoid fall and the measuring of the force applied to the arachnoid during the surgical procedure. It consists of two main parts: the anatomical module and the tank system. Moreover, it was designed to be modular and customizable. Finally, it is equipped with a pressure sensor that allows the indirect estimation of the force applied to the arachnoid membrane. It was fabricated using AM and Rapid Prototyping technologies with mold casting. FFF technology with PLA was used for bones, TPU for cartilage, and soft silicone was used to mimic the properties of the skin and the mucosa. Molds for silicone casting were obtained using PLA patterns. ABS was used for the structure of the tank. The arachnoid membrane was mimicked with polymeric film and the CSF was reproduced with distilled water. Preliminary tests demonstrated a strong linear correlation between pressure and force on the membrane (R^2 of 0.972 and sensitivity of 1.289 N/kPa). Then, the model was evaluated during a hands-on session that involved 11 experienced international surgeons who simulated a pituitary adenoma resection procedure, using pieces of boiled egg white to emulate the tumor. During the session, force values and surgeon's feedback were collected. Results on force are aligned with the literature and allowed the identification of three working areas (Safe, Warning, and CSF Leak), which can be used to evaluate the trainee's performance. Finally, the innovative features of the model received valuable feedback from the surgeons. In particular, the arachnoid and the consistency of the pituitary tumor are well mimicked.

Future research will be focused on improving the thickness and rigidity of the arachnoid and on how to achieve different consistencies for the pituitary adenoma. It will also be interesting to implement bleeding effects and more colors and textures to make the experience more vivid, as suggested by the surgeons. Furthermore, new sensors will be integrated into the training model to provide more data about the surgeon's performance. Nowadays, the gold standard is still training with cadaveric heads, which have the advantage of better anatomical realism, but their low availability, together with the fact that they are not suitable for repetitive training experiences, nor do they have the tumor to be removed makes them expensive training solutions. The objective is to develop a training model that can be an alternative to classical training experience and can provide objective data on the expertise of the surgeon before entering the operating room.

CRediT authorship contribution statement

Giacomo Santona: Writing – review & editing, Writing – original draft, Visualization, Validation, Resources, Formal analysis, Conceptualization. **Antonio Fiorentino:** Writing – review & editing, Validation, Resources, Formal analysis, Conceptualization. **Francesco Doglietto:** Writing – review & editing, Validation, Resources, Conceptualization. **Mauro Serpelloni:** Writing – review & editing, Validation, Resources, Formal analysis, Conceptualization.

Ethical approval statement

In accordance with the ethical standards set for this research, an ethics committee review and approval were not required for this study, as it is a pilot study on the usability of the proposed system. Furthermore, no clinical studies or similar were conducted. All participants provided informed verbal consent to participate in the study.

Data statement

The data supporting this study's findings are available from the corresponding author upon reasonable request.

Declaration of generative AI and AI-assisted technologies in the writing process

During the preparation of this work the authors used "DeepL Write" and "Grammarly" to improve language and readability. After using these services, the authors reviewed and edited the content as needed and take full responsibility for the content of the publication.

Fundings

This work was supported by Università degli Studi di Brescia.

Declaration of competing interest

The authors declare that they have no known competing financial interests or personal relationships that could have appeared to influence the work reported in this paper.

Acknowledgments

We would like to thank the laboratory technician Mr. Cristian Magrini for his support and guidance in the preparation of the experimental setup for characterization tests.

Appendix A. Supplementary data

Supplementary data to this article can be found online at https://doi.org/10.1016/j.heliyon.2025.e43380.

References

[1] F. Doglietto, D.M. Prevedello, J.A. Jane, J. Han, E.R. Laws, A brief history of endoscopic transsphenoidal Surgery—from Philipp Bozzini to the first world congress of endoscopic skull base surgery, Neurosurg. Focus 19 (2005) 1–6, https://doi.org/10.3171/foc.2005.19.6.4.
[2] S. Melmed, D.L. Kleinberg, V. Bonert, M. Fleseriu, Acromegaly: assessing the disorder and navigating therapeutic options for treatment, Endocr. Pract. Off. J. Am. Coll. Endocrinol. Am. Assoc. Clin. Endocrinol. 20 (Suppl 1) (2014) 7–17, https://doi.org/10.4158/EP14430.RA, 18–20.
[3] K. Kenan, A. İhsan, O. Dilek, C. Burak, K. Gurkan, C. Savas, The learning curve in endoscopic pituitary surgery and our experience, Neurosurg. Rev. 29 (2006) 298–305, https://doi.org/10.1007/s10143-006-0033-9.
[4] N. Choudhury, N. Gélinas-Phaneuf, S. Delorme, R. Del Maestro, Fundamentals of neurosurgery: virtual reality tasks for training and evaluation of technical skills, World Neurosurg. 80 (2013) e9–e19, https://doi.org/10.1016/j.wneu.2012.08.022.
[5] G. Santona, A. Madoglio, D. Mattavelli, M. Rigante, M. Ferrari, L. Lauretti, P. Mattogno, C. Parrilla, P. De Bonis, J. Galli, A. Olivi, M.M. Fontanella, A. Fiorentino, M. Serpelloni, F. Doglietto, Training models and simulators for endoscopic transsphenoidal surgery: a systematic review, Neurosurg. Rev. 46 (2023) 248, https://doi.org/10.1007/s10143-023-02149-3.
[6] K. Hartmann, K.-P. Stein, B. Neyazi, I.E. Sandalcioglu, First in vivo visualization of the human subarachnoid space and brain cortex via optical coherence tomography, Ther. Adv. Neurol. Disord. 12 (2019) 1756286419843040, https://doi.org/10.1177/1756286419843040.
[7] A. Khasawneh, R. Garling, C. Harris, Cerebrospinal fluid circulation: what do we know and how do we know it? Brain Circ. 4 (2018) 14, https://doi.org/10.4103/bc.BC_3_18.
[8] D.R. Walsh, Z. Zhou, X. Li, J. Kearns, D.T. Newport, J.J.E. Mulvihill, Mechanical properties of the cranial meninges: a systematic review, J. Neurotrauma 38 (2021) 1748–1761, https://doi.org/10.1089/neu.2020.7288.
[9] L. Sakka, G. Coll, J. Chazal, Anatomy and physiology of cerebrospinal fluid, Eur. Ann. Otorhinolaryngol. Head Neck Dis. 128 (2011) 309–316, https://doi.org/10.1016/j.anorl.2011.03.002.
[10] M. Salmi, Additive manufacturing processes in medical applications, Materials 14 (2021) 191, https://doi.org/10.3390/ma14010191.
[11] J. Chen, K. Wang, C. Zhang, B. Wang, An efficient statistical approach to design 3D-printed metamaterials for mimicking mechanical properties of soft biological tissues, Addit. Manuf. 24 (2018) 341–352, https://doi.org/10.1016/j.addma.2018.10.007.
[12] C.J. Darling, C. Curtis, B.J. Sciacca, K. Sarkar, D.A. Smith, Fused filament fabrication of complex anatomical phantoms with infill-tunable image contrast, Addit. Manuf. 52 (2022) 102695, https://doi.org/10.1016/j.addma.2022.102695.
[13] A. Fiorentino, C. Piazza, E. Ceretti, Anti-migration enhanced tracheal stent design, rapid manufacturing and experimental tests, Rapid Prototyp. J. 22 (2016) 178–188, https://doi.org/10.1108/RPJ-06-2014-0072.
[14] A. Colpani, A. Fiorentino, E. Ceretti, 3D printing for health & wealth: fabrication of custom-made medical devices through additive manufacturing. https://doi.org/10.1063/1.5034998, 2018.

[15] J. Lin, Z. Zhou, J. Guan, Y. Zhu, Y. Liu, Z. Yang, B. Lin, Y. Jiang, X. Quan, Y. Ke, T. Xu, Using three-dimensional printing to create individualized cranial nerve models for skull base tumor surgery, World Neurosurg. 120 (2018) e142–e152, https://doi.org/10.1016/j.wneu.2018.07.236.
[16] N. Harada, K. Kondo, C. Miyazaki, J. Nomoto, S. Kitajima, M. Nemoto, H. Uekusa, M. Harada, N. Sugo, Modified three-dimensional brain model for study of the trans-sylvian approach, Neurol. Med.-Chir. 51 (2011) 567–571, https://doi.org/10.2176/nmc.51.567.
[17] T. Okuda, K. Kataoka, A. Kato, Training in endoscopic endonasal transsphenoidal surgery using a skull model and eggs, Acta Neurochir. 152 (2010) 1801–1804, https://doi.org/10.1007/s00701-010-0728-0 (Wien).
[18] T. Okuda, J. Yamashita, M. Fujita, H. Yoshioka, T. Tasaki, A. Kato, The chicken egg and skull model of endoscopic endonasal transsphenoidal surgery improves trainee drilling skills, Acta Neurochir. 156 (2014) 1403–1407, https://doi.org/10.1007/s00701-014-2035-7.
[19] D.C. Engel, A. Ferrari, A.-J. Tasman, R. Schmid, R. Schindel, S.R. Haile, L. Mariani, J.-Y. Fournier, A basic model for training of microscopic and endoscopic transsphenoidal pituitary surgery: the egghead, Acta Neurochir. 157 (2015) 1771–1777, https://doi.org/10.1007/s00701-015-2544-z. ; discussion 1777.
[20] G. Wen, Z. Cong, K. Liu, C. Tang, C. Zhong, L. Li, X. Dai, C. Ma, A practical 3D printed simulator for endoscopic endonasal transsphenoidal surgery to improve basic operational skills, childs nerv, Syst. ChNS Off. J. Int. Soc. Pediatr. Neurosurg. 32 (2016) 1109–1116, https://doi.org/10.1007/s00381-016-3051-0.
[21] C.-Y. Ding, X.-H. Yi, C.-Z. Jiang, H. Xu, X.-R. Yan, Y.-L. Zhang, D.-Z. Kang, Z.-Y. Lin, Development and validation of a multi-color model using 3-dimensional printing technology for endoscopic endonasal surgical training, Am. J. Transl. Res. 11 (2019) 1040–1048.
[22] P. Gallet, J. Rebois, D.-T. Nguyen, R. Jankowski, M. Perez, C. Rumeau, Simulation-based training in endoscopic endonasal surgery: assessment of the cyrano simulator, Eur. Ann. Otorhinolaryngol. Head Neck Dis. 138 (2021) 29–34, https://doi.org/10.1016/j.anorl.2020.08.012.
[23] G. Santona, T. Fapanni, A. Fiorentino, F. Doglietto, M. Serpelloni, Preliminary study on a 3D printed sensorized probe to characterize pituitary adenoma hardness. https://doi.org/10.1109/MetroInd4.0IoT57462.2023.10180133, 2023.
[24] G. Santona, A. Fiorentino, F. Doglietto, M. Serpelloni, A novel 3D printed sensorized surgical instrument to characterize pituitary adenoma: development and initial validation, in: 2024 IEEE Int. Workshop Metrol, Ind. 40 IoT MetroInd40 IoT, 2024, pp. 7–11, https://doi.org/10.1109/MetroInd4.0IoT61288.2024.10584245.
[25] G. Santona, T. Fapanni, A. Fiorentino, F. Doglietto, M. Serpelloni, Preliminary study of a sensorized system for real-time feedback for arachnoid collapse during neurosurgical training, in: 2023 IEEE Int. Workshop Metrol. Ind. 40 Iot MetroInd40IoT, 2023, pp. 233–238, https://doi.org/10.1109/MetroInd4.0IoT57462.2023.10180173.
[26] J.H. Thomas, Fluid dynamics of cerebrospinal fluid flow in perivascular spaces, J. R. Soc. Interface 16 (2019) 20190572, https://doi.org/10.1098/rsif.2019.0572.
[27] A.A. AlQahtani, A.A. Albathi, O.M. Alhammad, A.S. Alrabie, Innovative real CSF leak simulation model for rhinology training: human cadaveric design, Eur. Arch. Oto-Rhino-Laryngol. Off. J. Eur. Fed. Oto-Rhino-Laryngol. Soc. EUFOS Affil. Ger. Soc. Oto-Rhino-Laryngol. - Head Neck Surg. 275 (2018) 937–941, https://doi.org/10.1007/s00405-018-4902-y.
[28] E.A. Christian, J. Bakhsheshian, B.A. Strickland, V.L. Fredrickson, I.A. Buchanan, M.H. Pham, A. Cervantes, M. Minneti, B.B. Wrobel, S. Giannotta, G. Zada, Perfusion-based human cadaveric specimen as a simulation training model in repairing cerebrospinal fluid leaks during endoscopic endonasal skull base surgery, J. Neurosurg. 129 (2018) 792–796, https://doi.org/10.3171/2017.5.JNS162982.
[29] D. Mattavelli, M. Ferrari, V. Rampinelli, A. Schreiber, B. Buffoli, A. Deganello, L.F. Rodella, M.M. Fontanella, P. Nicolai, F. Doglietto, Development and validation of a preclinical model for training and assessment of cerebrospinal fluid leak repair in endoscopic skull base surgery, Int. Forum Allergy Rhinol. 10 (2020) 89–96, https://doi.org/10.1002/alr.22451.
[30] A. AlQahtani, A. Albathi, P. Castelnuovo, F. Alfawwaz, Cerebrospinal fluid leak repair simulation model: face, content, and construct validation, Am. J. Rhinol. Allergy 35 (2021) 264–271, https://doi.org/10.1177/1945892420952262.
[31] M.A. Masalha, K.K. VanKoevering, O.S. Latif, A.R. Powell, A. Zhang, K.H. Hod, D.M. Prevedello, R.L. Carrau, Simulation of cerebrospinal fluid leak repair using a 3-Dimensional printed model, Am. J. Rhinol. Allergy 35 (2021) 802–808, https://doi.org/10.1177/19458924211003537.
[32] V.A. Chandankhede, S.K. Singh, R. Roy, S. Goyal, M.S. Sridhar, M.S. Gill, Transnasal transsphenoidal approach for pituitary tumors: an ENT perspective, Indian J. Otolaryngol. Head Neck Surg. 72 (2020) 239–246, https://doi.org/10.1007/s12070-020-01803-2.
[33] J.R. Bekeny, P.J. Swaney, R.J. Webster III, P.T. Russell, K.D. Weaver, Forces applied at the skull base during transnasal endoscopic transsphenoidal pituitary tumor excision, J. Neurol. Surg. Part B Skull Base 74 (2013) 337–341, https://doi.org/10.1055/s-0033-1345108.